Journal of Structural Chemistry. Vol. 59, No. 1, pp. 36-42, 2018.

CRYSTALLOGRAPHIC AND COMPUTATIONAL STUDIES ON N-FURFURYL-N-(3-HYDROXYBENZYL)AMINE AND N-FURFURYL-N-(4-HYDROXYBENZYL)AMINE

E. Sathiyaraj[1,2], S. Thirumaran[1], and S. Ciattini[3]

Crystal structures of N-furfuryl-N-(3-hydroxybenzyl)amine (**1**) and N-furfuryl-N-(4-hydroxybenzyl)amine (**2**) are reported. The furyl ring is coplanar with the C–N–C plane in **1** and perpendicular to the C–N–C plane in **2**. Intermolecular O–H···N and C–H···O hydrogen bonds stabilize the crystal structures and play a crucial role in crystal packing. In addition, the molecular geometry and molecular vibrations are calculated using the DFT/B3LYP method with the 6-31G(*d*,*p*) basis set and the calculated geometrical parameters are correlated with the corresponding experimental data. The obtained HOMO and LUMO energies are negative, indicating that the compounds are in the stable state. FT-IR spectra of compounds **1** and **2** are measured in order to elucidate the spectroscopic properties of the compounds in the spectral range 4000-500 cm^{-1}. The recorded FT-IR spectral measurements are further supported by spectral simulations.

DOI: 10.1134/S0022476618010067

Keywords: crystal structures, DFT, HOMO-LUMO, vibrational spectra.

INTRODUCTION

The five-membered heterocyclic furyl ring system commonly occurs in many natural products. Heterocyclic compounds are important due to their pharmacological, agrochemical, and biological activities. Due to a higher production of furfurylamine and its derivatives compared to benzylamine and its derivatives, furfurylamine and its derivatives are used to replace benzylamine and its derivatives on an industrial scale for manufacturing fertilizers [1] and drugs [2]. Schiff bases can be obtained in good yields and high purity by a simple condensation reaction of primary amines with aldehydes (or) ketones [3]. The reduction of Schiff bases yielded amines. The synthesis of heterocyclic compounds and their anticancer, antimoebic, antibacterial, antifungal, antiviral, anti-HIV [4, 5] and tuberculosis [6] activities have also been reported. The study of amines and their derivatives is important due to the presence of amines in natural products and nucleic acids [7]. Amines are widely used in many industries as basic intermediates for the preparation of fine chemicals, pharmaceuticals, agro chemicals, etc. [8]. Particularly, secondary amines are extremely important pharmacophores in numerous biologically active compounds, which have greatly been touted in the area of drug discovery [9]. In view of the growing importance of amines in biological field and in order to study hydrogen bonding interactions due to the presence of OH and NH groups in the compounds, the single crystal structural analysis of compounds **1** and **2** has been carried out. In addition, the molecular geometry and molecular

[1]Department of Chemistry, Annamalai University, Annamalainagar, India; chemsathya2010@gmail.com. [2]Department of Chemistry, Kalasalingam University, Krishnan koil, India. [3]Centro di Cristallografia Strutturale, Polo Scientifio di Sesto Fiorentino, Firenze, Italy. The text was submitted by the authors in English. *Zhurnal Strukturnoi Khimii*, Vol. 59, No. 1, pp. 44-50, January-February, 2018. Original article submitted February 4, 2016; revised May 24, 2016.

vibrations have been calculated using the DFT/B3LYP method with the 6-31G(*d*,*p*) basis set and the calculated geometrical parameters are correlated with the corresponding experimental data.

EXPERIMENTAL

Materials and methods. All chemicals were commercially available analytical grade materials and used as supplied without further purification. FT-IR spectra were recorded on a thermo scientific NICOLET iS5 spectrophotometer. The spectra were taken suitably as potassium bromide discs of the compounds.

Crystal structure determination and structure refinement. Details of the crystal data, data collection and structure refinement parameters are summarized in Table 1. The intensity data were collected at ambient temperature (293(2) K) for compound **1** and 150 K for compound **2** on an Oxford Diffraction Xcalibur 3 (with CCD) diffractometer using graphite-monochromated MoK_α radiation ($\lambda = 0.71069$ Å and $\lambda = 0.71073$ Å). The structures were solved by SHELXS-97 [10] and refined by the full matrix least squares technique with SHELXL-97 [11]. All the non-hydrogen atoms were refined anisotropically and hydrogen atoms were refined isotropically.

Computational procedure. The DFT calculation with the B3LYP hybrid function at the 6-31 basis set G(*d*,*p*) [12] was performed by the Berny method. All theoretical calculations were made by the Gaussian03W [13] software package. The optimized molecular geometry, theoretical IR spectra, and the molecular orbital descriptions (HOMO, LUMO) for the title compounds were obtained from the computational calculations.

Preparation of N-furfuryl-N-substituted benzylamine. Furfurylamine (4.6 mmol) and substituted benzaldehydes (3-OH, 4-OH) (5.1 mmol) were dissolved in methanol (30 ml) and the solution was stirred for 2 h at room temperature. The

TABLE 1. Crystal Data, Data Collection and Structure Refinement for Compounds **1** and **2**

Compound	**1**	**2**
Empirical formula	$C_{12}H_{13}N_2O_4$	$C_{12}H_{13}N_2O_4$
Formula weight	203.23	203.23
Temperature, K	293(2)	150(2)
Wavelength, Å	0.71069	0.71073
Crystal system	Monoclinic	Orthorhombic
Space group	*C*2/*c*	$P2_12_12_1$
Unit cell dimensions *a*, *b*, *c*, Å; β, deg	20.659(5), 7.929(5), 17.176(5); 132.620(5)	5.4506(5), 13.2560(10), 13.7800(10); 90
Volume, *V*, Å^3	2070.4(15)	995.65(14)
Z; Calculated density, g/cm^3	8; 1.304	4; 1.356
Absorption coefficient μ, cm^{-1}	0.089	0.093
F(000)	864	432
Crystal size, mm	0.30×0.20×0.15	0.4×0.35×0.30
θ Range, deg.	4.454 to 32.697	4.30 to 32.4
Limiting indices	$-29 \le h \le 31$, $-10 \le k \le 12$, $-25 \le l \le 25$	$-7 \le h \le 5$, $-19 \le k \le 11$, $-20 \le l \le 19$,
Reflections collected / unique	10222 / 3471	5599 / 1639
Completeness to θ	25.24	32.46
Max. and min. transmission	1.00000 and 0.80904	1.00000 and 0.75000
Data / restraints / parameters	3471 / 0 / 188	2935 / 0 /188
Goodness-of-fit on F^2	1.011	1.038
Final *R* indices [$I > 2\sigma(I)$]	$R_1 = 0.0537$, $wR_2 = 0.1118$	$R_1 = 0.0484$, $wR_2 = 0.1039$
R indices (all data)	$R_1 = 0.1023$, $wR_2 = 0.1389$	$R_1 = 0.0643$, $wR_2 = 0.1165$
Largest diff. peak and hole	0.183, –0.219	0.278, –0.218

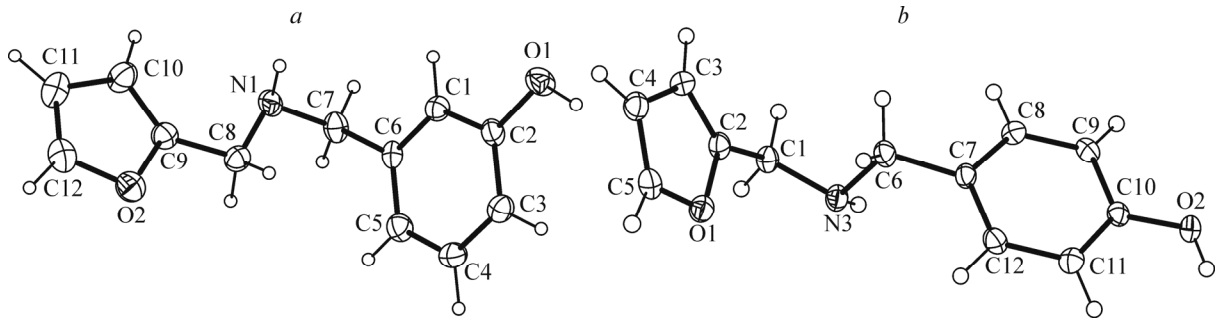

Fig. 1. ORTEP diagram of compounds **1** (*a*) and **2** (*b*).

solvent was removed by evaporation. The resulting yellow oil was dissolved in a methanol-dichloromethane solvent mixture (1:1, 20 ml) and sodium borohydride (13.8 mmol) was added slowly and stirred for 2 h at 5 °C. The mixture was stirred at room temperature for 20 h. After evaporation of the solvent, the resulting viscous liquid was washed with water and dichloromethane was added in order to extract the product. Evaporation of the organic layer gave N-furfuryl-N-substituted benzylamine as yellow oil. Suitable single crystals for the X-ray structural analysis were obtained by repeated recrystallization from ethanol for **1** and dichloromethane for **2**.

RESULTS AND DISCUSSION

Structure analysis. The ORTEP diagrams of **1** and **2** are shown in Fig. 1. Selected bond distances and bond angles are listed in Table 2. Bond lengths of compounds **1** and **2** are in the normal range (mean: C–C = 1.381(2) Å, C–O = 1.365(2) Å, and C–N = 1.466(2) Å for compound **1** and C–C = 1.407 Å, C–O = 1.364(2) Å, and C–N = 1.476(2) Å for compound **2**). The bond parameters associated with phenyl and furyl rings are also normal. In compound **1**, the furyl ring is coplanar with the C7–N1–C8 plane (the dihedral angle of the furyl ring and C7–N1–C8 planes is 5.96° and the torsion angle C9–C8–N1–C7 = 175.41°). However, in compound **2**, the furyl ring is perpendicular to the C1–N3–C6 plane (the dihedral angle of the furyl ring and C1–N3–C6 planes is 89.27°). The phenyl ring deviates from the C–N–C plane with dihedral angles of 76.56° and 69.47° for compounds **1** and **2**, respectively.

In the crystal structure of compound **1**, the O–H···N intermolecular interaction provides a linear chain structure (Fig. 2*a*). The H···N separation is short (H1···N1 = 1.779 Å). Furthermore, two O···H interactions lead to the 32-membered macrocyclic ring. One of the O···H distances (O1···H12 = 2.475 Å) is short (Fig. 2*b*). It may be assumed that these two hydrogen atoms are more acidic in terms of the identities of their adjacent atoms [14]. The crystal structure of **2** is stabilized by intermolecular O–H···N and C–H···O interactions (Fig. 3*a*, *b*). The two C–H···O interactions in compound **2** are linked to the same acceptor O atom. Both O···H distances are almost equal (O2···H3 = 2.569 Å and O2···H12 = 2.583 Å). The C–H···O intermolecular hydrogen bonding with another oxygen atom (furyl) is also observed (O1···H5 = 2.623 Å). In addition to the C–H···O interactions, the amine N atom is linked with O–H of another molecule. The H···N distance is 1.946 Å. The packing is further stabilized by two additional edge-to-face C–H···π interactions. The C–H···Cg1 and

TABLE 2. Hydrogen Bond Geometry for Compounds **1** and **2**

Interactions	D–H	H···A	D···A	D–H···A	Interactions	D–H	H···A	D···A	D–H···A
Compound **1**					Compound **2**				
O(1)–H(1)···N(1)	0.99	1.78	2.7642	173	O(2)–H(3)···N(3)	0.86	1.95	2.787	166
C(1)–H(1)···O(1)	0.97	2.58	3.4688	153	C(3)–H(3)···O(1)	0.95	2.56	3.412	148
C(12)–H(12)···O(1)	0.98	2.48	3.3922	156	C(12)–H(12)···O(1)	0.99	2.58	3.349	134
					C(5)–H(5)···O(1)	0.94	2.62	3.388	139

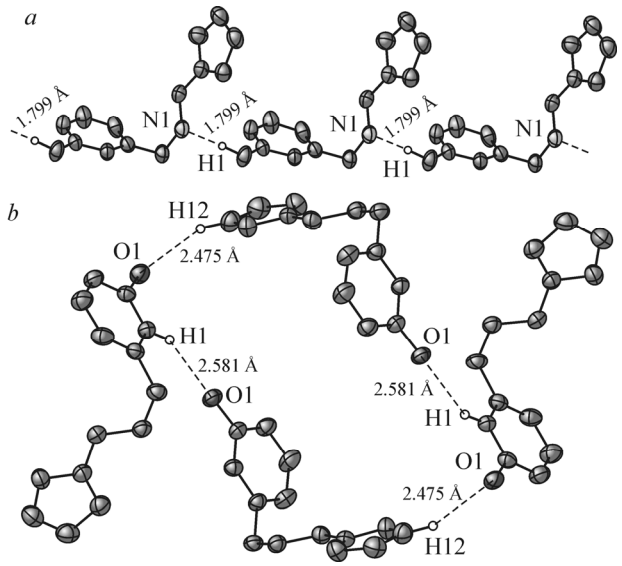

Fig. 2. Supramolecular linear chain formation *via* the O–H···N hydrogen interaction in compound **1** (*a*); perspective view of the 32-membered macrocyclic ring present in compound **1** (*b*).

C–H···Cg2 distances are 2.665 Å and 2.911 Å, respectively (Fig. 3*c* and Table 2). In both compounds, intermolecular O–H···N hydrogen bonds form a C(9) and C(10) chain in the unit cell for **1** and **2**, respectively (Figs. 2*a* and 3*a*).

Optimized geometry. A comparison of the experimental bond parameters with the calculated values shows that the largest bond length difference is 0.14 Å and 0.11 Å for C–C distances in compounds **1** and **2**, respectively and the bond angle difference is 3.8° (C11–C12–O2) and 2.7° (N1–C1–C6) in compounds **1** and **2**, respectively. As for the largest difference in the bond lengths and bond angles, it can result from two reasons: (i) all the calculated data are for the molecule in the gas phase, while the experimental data are for the molecules in the solid state, and (ii) various hydrogen bonding interactions are observed in the solid state but the calculated values are for the isolated molecule. The C–C bond lengths in the phenyl rings lie between 1.372-1.399 Å (DFT) and 1.374(3)-1.385(2) Å (XRD) for compound **1** and 1.393-1.514 Å (DFT) and 1.391(2)-1.503(3) Å (XRD) for compound **2**, and the bond lengths are in between the normal values for single (1.54 Å) and double (1.33 Å) bonds [15].

HOMO-LUMO. The HOMO-LUMO and HOMO-1-LUMO+1 energy values are 6.1960 eV and 6.5927 eV for **1** and 5.7644 eV and 6.1612 eV for **2**, respectively. HOMO and LUMO represent the ability to donate and accept an electron, respectively. For compound **1**, the π electron density of HOMO is localized fully and partially on the furyl and phenyl rings, respectively, and the electron density of HOMO-1 is localized fully only on the phenyl ring, whereas the electron density on LUMO and LUMO+1 are localized overall the molecule.

In the case of HOMO and HOMO-1, the electron density is localized overall the molecule in compound **2**, whereas in LUMO, the electron density is localized only on the phenyl ring, and LUMO+1 is fully localized on the phenyl ring and partially on the furyl ring. The HOMO-LUMO energy gap in compound **1** is larger than that found in compound **2**. This indicates that compound **1** is more stable compared to compound **2**. Moreover, the lower HOMO-LUMO energy gap explains the eventual charge transfer interactions taking place within the molecule.

Molecular electronic potential (MEP). MEPs of compounds **1** and **2** were determined using the B3LYP/6-31G(*d*,*p*) method. This is a very useful descriptor to understand the partial charges and chemical reactivity of the molecule [16]. The MEP studies of **1** and **2** show that the negative charge covers the OH oxygen atoms and furyl groups and the positive charge is localized on the hydrogen atoms of OH and NH groups. Oxygen is the the most reactive part in the molecule due to the presence of higher electronegativity on O atoms of OH and furyl groups.

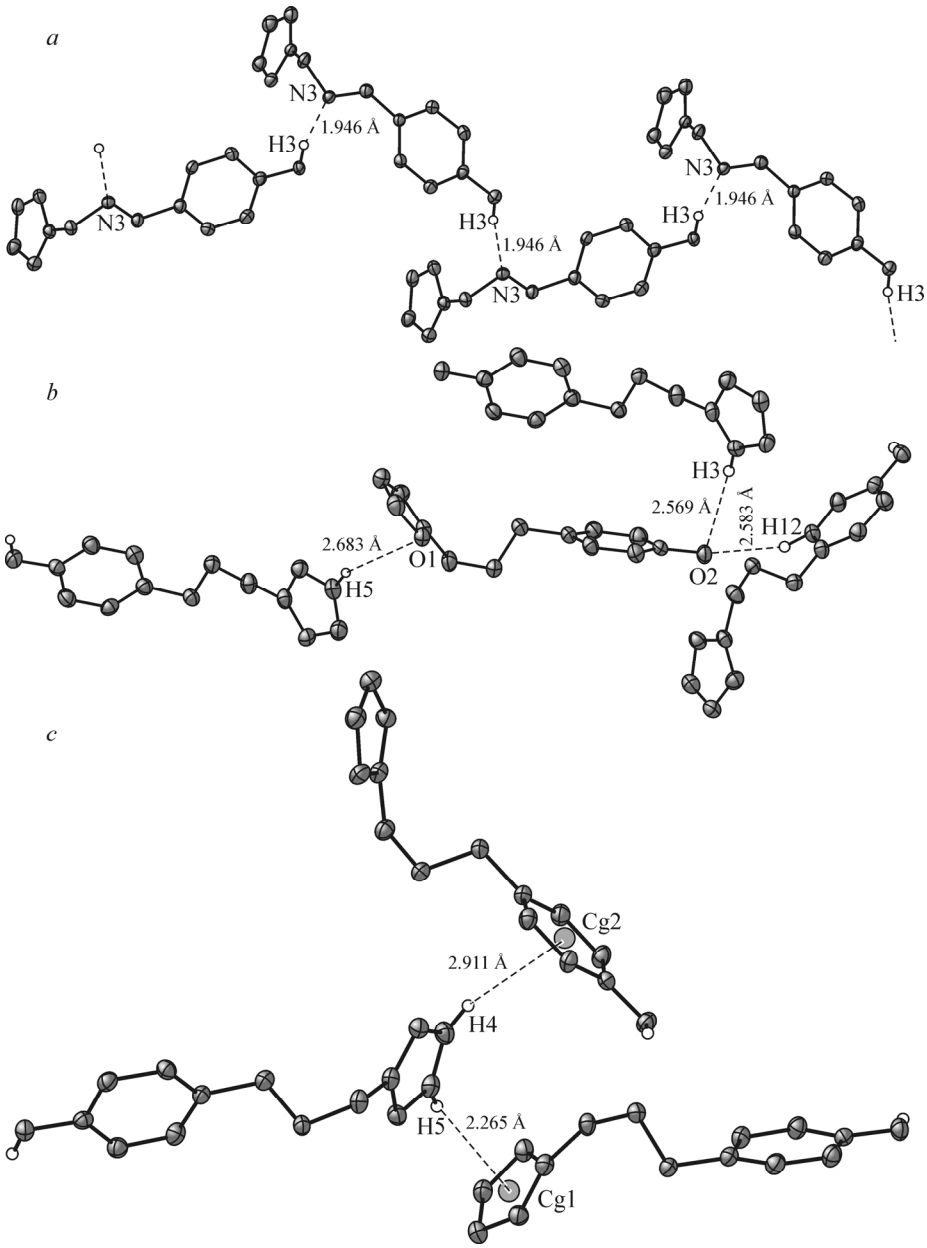

Fig. 3. View of compound **2** showing O–H…N chain interactions (*a*); view of compound **2** showing C–H…O interactions (*b*); view of edge-to-face interactions between the adjacent phenyl and furyl moieties of compound **2** (*c*).

FT-IR spectra. Vibrational frequencies calculated at the B3LYP/6-31G(*d,p*) level of theory were scaled by the dual scaling factor (<1800 cm for 0.9927 cm^{-1} and >1800 cm for 0.9659 cm^{-1}) for this method [17, 18].

Selected primary calculated harmonic frequencies and the experimental data are listed in Table 3. Due to the possible mixing of several bands in the C–N stretching frequency region [19], the C–N stretching vibrations are assigned with the help of computational studies. The C–N stretching vibration coupled with the N–H scissoring one is moderately to strongly active in the region 1275±55 cm^{-1} [20]. The bands observed at 1259 cm^{-1} for **1** and 1250 cm^{-1} for **2** are assigned to C–N stretching vibrations, and these stretching frequencies show excellent agreement with the theoretically calculated values (1258 cm^{-1} and 1247 cm^{-1} for **1** and **2**, respectively). The N–H stretching vibration appears strongly and broadly in the region 3500-3300 cm^{-1} [21]. In this study, the N–H frequencies are observed at 3284 cm^{-1} and 3305 cm^{-1} for **1** and **2**, respectively. The O–H frequencies are observed at 3441 cm^{-1} and 3450 cm^{-1} [22]. Large differences observed between the calculated and experimental O–H stretching vibrations are mainly due to O–H···N interactions in the solid state.

TABLE 3. Important Infrared Spectral Data of Compounds **1** and **2**

Functional group	Compound **1**		Compound **2**	
	Experimental	B3LYP/6-31G(*d*,*p*)	Experimental	B3LYP/6-31G(*d*,*p*)
C–N	1281	1297	1250	1288
Furyl	3111	3127	3116	3130
N–H	3284	3164	3305	3372
O–H	3441	3668	3450	3670

CONCLUSIONS

Crystal structures of **1** and **2** were analysed by single crystal X-ray diffraction. The crystal structure is stabilized by intermolecular C–H···O and O–H···N hydrogen bonds in which the intermolecular O–H···N hydrogen bond generates a C9 and C10 chain motif in compounds **1** and **2**. Density functional theory calculations of the structures, vibrational spectra, HOMO-LUMO, and MEP analyses of compounds **1** and **2** were also carried out. The equilibrium geometry is obtained at the B3LYP/6-31G(*d*,*p*) level for both bond lengths and bond angles. The vibrational frequency analysis by the B3LYP/6-31G(*d*,*p*) method agrees satisfactorily with the experimental results. Any differences observed between the experimental and computed values may be due to the fact that the computations were performed for a single molecule in the gas phase, whereas the experimental values were recorded in the solid phase in the presence of intermolecular interactions. The lower HOMO-LUMO band gap supports the bioactive property of the compounds.

The crystallographic data for the structural analysis of compounds **1** and **2** have been deposited with the Cambridge Crystallographic Data Centre, CCDC No. for **1** is 1025267 and 1025410 for **2**. Copy of this information may be obtained free of charge from the Director, CCDC, 12 Union Road, Cambridge CB2 1EZ, UK (Tel.:þ44 (0) 1223 762911; E-mail: kamila@ccdc.cam.ac.uk).

REFERENCES

1. N. Aggarwal, R. Kumar, P. Dureja, and D. S. Rawat, *J. Agric. Food Chem*., **57**, 8520-8525 (2009).
2. K. Florey, *Elsevier*, **18**, 153 (1990).
3. S. Bilge, Z. Kili, Z. Hayvali, T. Kelek, and S. Safran, *J. Chem. Sci*., **121**, 989-1001 (2009).
4. A. M. Asiri and S. A. Khan, *Molecules*, **15**, 4784-4791 (2010).
5. S. N. Pandeya, D. Sriram, G. Nath, and E. De Clercq, *Arzneim. Forsch*., **50**, 55-59 (2000).
6. T. Aboul-Fadl, H. A. Abdel-Aziz, M. K. Abdel-Hamid, T. Elsaman, J. Thanassi, and M. J. Pucci, *Molecules*, **16**, 7864-7879 (2011).
7. S. S. Insaf and D. Twitiak, *Synthesis*, **3**, 435-440 (1999).
8. D. F. Berry and S. A. Royl, *Soil Sci. Soc. Am. J*., **48**, 565-569 (1984).
9. S. Migliari, R. Fender, and M. Méndez, *Science*, **297**, 1673-1676 (2002).
10. G. M. Sheldrick, *SHELXS-97, Program for Crystal Structure Determination*, University of Göttingen, Germany (1997).
11. G. M. Sheldrick, *SHELXL-97, Program for the Refinement of Crystal Structure*, University of Göttingen, Germany (1997).
12. C. Peng, P. Y. Ayala, H. B. Schlegel, and M. J. Frisch, *J. Comput. Chem*., **17**, 49-56 (1996).
13. M. J. Frisch, G. W. Trucks, H. B. Schlegel, G. E. Scuseria, M. A. Robb, J. R. Cheeseman, J. A. Montgomery Jr., T. Vreven, K. N. Kudin, J. C. Burant, J. M. Millam, S. S. Iyengar, J. Tomasi, V. Barone, B. Mennucci, M. Cossi, G. Scalmani, N. Rega, G. A. Petersson, H. Nakatsuji, M. Hada, M. Ehara, K. Toyota, R. Fukuda, J. Hasegawa, M. Ishida, T. Nakajima, Y. Honda, O. Kitao, H. Nakai, M. Klene, X. Li, J. E. Knox, H. P. Hratchian, J. B. Cross,

C. Adamo, J. Jaramillo, R. Gomperts, R. E. Stratmann, O. Yazyev, A. J. Austin, R. Cammi, C. Pomelli, J. W. Ochterski, P. Y. Ayala, K. Morokuma, G. A. Voth, P. Salvador, J. J. Dannenberg, V. G. Zakrzewski, S. Dapprich, A. D. Daniels, M. C. Strain, O. Farkas, D. K. Malick, A. D. Rabuck, K. Raghavachari, J. B. Foresman, J. V. Ortiz, Q. Cui, A. G. Baboul, S. Clifford, J. Cioslowski, B. B. Stefanov, G. Liu, A. Liashenko, P. Piskorz, I. Komaromi, R. L. Martin, D. J. Fox, T. Keith, M. A. Al-Laham, C. Y. Peng, A. Nanayakkara, M. Challacombe, P. M. W. Gill, B. Johnson, W. Chen, M. W. Wong, C. Gonzalez, and J. A. Pople, *Gaussian 03, Revision B.04*, Gaussian, Inc., Pittsburgh PA (2003).

14. W. T. A. Harrison, H. S. Yathirajan, B. K. Sarojini, B. Narayana, and H. G. Anilkumar, *Acta Crystallogr. C*, **61**, o728 (2005).
15. Y. S. Mary, K. Raju, I. Yildiz, O. Temiz-Arpaci, H. I. S. Nogueira, C. M. Granadeiro, and C. Van Alsenoy, *Spectrochim. Acta A*, **96**, 617-625 (2012).
16. E. Scrocco and J. Tomasi, *Adv. Quantum. Chem*., **11**, 115-121 (1978).
17. *NIST Chemistry Webbook, IR database*; http://srdata.nist.gov/cccbdb.
18. M. D. Halls, J. Velkovski, and H. B. Schlegel, *Theor. Chem. Acc*., **105**, 413-421 (2001).
19. M. Silverstein, G. C. Basselar, and C. Morill, *Spectrometric Identification of Organic Compounds*, Wiley, New York (1981).
20. N. P. G. Roeges, *A Guide to the Complete Interpretation of Infrared Spectra of Organic Structures*, Wiley, New York (1994).
21. Y. Erdogdu, M. T. Gulluoglu, and S. Yurdakul, *J. Mol. Struct*., **889**, 361-370 (2008).
22. Y. Erdogdu and M. T. Gulluoglu, *Spectrochim. Acta A*, **74**, 162-167 (2009).